Enhancing the Force Transparency of Time Domain Passivity Approach: Prescient Energy Reflection

Michael Panzirsch[1*], Harsimran Singh[1], Jee-Hwan Ryu[2], Christian Ott[1,3]

***Abstract*—The Time Domain Passivity Approach (TDPA) was developed to guarantee passivity while avoiding conservative constant controller parametrization. For this sake, the TDPA applies adaptive damping to dissipate excessive energy resulting from communication delay in bilateral teleoperation setups. Despite its advantages such as model-independent system observation and control or modularity, the transparency in TDPA is limited by two major artifacts: position drift and jitter in the force feedback signal. While a large variety of extensions have been proposed tackling the first issue, the latter received less attention since its solution is considerably more challenging. Recently, a concept with prescient energy reflection was proposed for the energy reflection-based TDPA (TDPA-ER) which significantly reduced force jitter in passive environments. Prescient energy reflection is feasible in TDPA-ER because the coupling controller is integrated within the passivity-controlled two-port subsystem. In this work, we demonstrate that prescient energy reflection can be applied to TDPA by leveraging the deflection-domain passivity approach. Experimental results with round-trip delays of up to 800 ms validate the potential and robustness of the proposed method considering metrics on force attenuation, perceived stiffness, as well as jitter properties.**

***Index Terms*—Teleoperation, Deflection-Domain Control**

I. Introduction

The nonlinearity in delayed coupled teleoperation systems is mostly tackled with energy-based control methods such as the wave variables approach [1] or the Time Domain Passivity Approach (TDPA, [2]) among others [3], [4]. The TDPA [5], [2], [6], [7] was shown to solve a variety of control challenges such as non-collocated force sensing [8], authority scaling [9] or delayed coupling [10], [11], [12] in robotic applications. After achieving IEEE standard performance [13], the majority of recent publications is dedicated to the transparency enhancement of TDPA regarding cross-dimensional [14] and other artifacts [15], haptic data reduction [16] or to particularly high delay (TDPA-HD, [17]). The first IEEE standard for delayed teleoperation IEEE 1918.1.1-2024 is based on an energy-reflection based TDPA (TDPA-ER, [13]).

Despite its large success, two types of artifacts affect the force and position transparency in TDPA controlled systems: A position drift (Issue 1) results from the adaptive velocity damping α of a passivity controller (PC1) dissipating excessive energy through variation of the delayed commanded velocity. Jitter (Issue 2.A) and drops (Issue 2.B) in the force feedback signal, both present in TDPA [5], TDPA-ER [13] as well as TDPA-HD [17], result from the adaptive force damping β (PC2) that varies the force (to dissipate excessive energy) on the opposite site of the communication channel.

Issue 1 was tackled via a variety of approaches ranging from position-drift compensation methods [18], [19] to novel TDPA concepts such as the TDPA-ER [20], [21], [22]. Still, more recently, positive aspects of position drift at high delay were presented in the space scenarios of [17], [23]. Therefore, and since the drift is not the focus of this work, no solution to solve Issue 1 is applied here.

To reduce the force jitter (Issue 2.A), the authors of [2] introduced a passive filter based on a virtual mass-spring damper system. Main drawbacks of this filter method are increased tuning efforts, hardware dependency and the introduction of an additional mass in the coupling causing phase shifts that limit the force transparency. This method focuses on the reduction of jitter, while force drops (Issue 2.B) cannot be prevented, as will be explained later in more detail. In contrast to [2] and [24], the proposed method can achieve zero force feedback attenuation at adequate speeds in passive environments.

Force drops (Issue 2.B) appear when no output power is available, even though power could suddenly exit to the input device. This happens predominantly, when changing motion directions of the input device during contacts such that PC2 has to dissipate the output power for the duration of one round-trip delay (RTD). I.e., in contrast to Issue 2.A, force drops do not appear when no power is left available, but when the information about available power hasn't arrived on the operator side yet. Such force drops were prevented for the first time in [21] for the TDPA-ER by presciently reflecting a part μ of the energy (μ-ER approach) that was sent to the robot (back to the input device side), assuming that this part of the energy would be reflected later anyways. Note that not the energy itself, but only the information that the energy should be available, is reflected back presciently. Thus, the energy is allocated presciently to the output on the input device side while it has to be prohibited to leave to the robot. This is enabled by TDPA-ER [21] since it ensures passivity not only of the communication channel (compare TDPA), but also

Manuscript received: August 1,2025; Revised: November 4, 2025; Accepted: December 10, 2025.

This paper was recommended for publication by Editor Haoyong Yu upon evaluation of the Associate Editor and Reviewers' comments.

This work was supported by the Bavarian Ministry of Economic Affairs, Regional Development and Energy, through the project SMiLE-AI (VLR-2506-0002).

*Corresponding author

[1]M. Panzirsch (michael.panzirsch@dlr.de), H. Singh (harsimran.singh@dlr.de) and C. Ott are with the Institute of Robotics and Mechatronics in the German Aerospace Center (DLR), Wessling, Germany.

[2]J.-H. Ryu (jhryu@kaist.ac.kr) is with the Department of Civil and Environmental Engineering, Korea Advanced Institute of Science & Technology, Seoul, Korea.

[3]C. Ott (christian.ott@tuwien.ac.at) is with the Automation and Control Institute, TU Wien, Vienna, Austria.

Digital Object Identifier (DOI): see top of this page.

	RTD range	Benefits	Limitations
TDPA-ER [13]	0ms-500ms	+ no drift due to avoidance of admittance-type PC + high coupling rigidity	− high coupling rigidity can limit perception with increasing delay − compatibility reduced due to integration of coupling controller
+μ-ER [21]		+ remove jitter and force drops on input device side + DDPA not required to ensure passivity	− potential lack of energy on robot side causing more jitter on robot side
+DDPA [21]		+ reduce overall jitter on robot side which is caused by delay and potentially μ-ER	
TDPA [2]	0ms-250ms	+ low implementation effort + compatibility	− drift due to admittance-type PC − critical drift during free motion at RTD >500ms − lower coupling rigidity − drift compensation methods insufficient at higher delay
+μ-ER, DDPA *[this work]*		+ μ-ER promises to reduce jitter and force drops on input device side	− DDPA required on robot side to ensure passivity
TDPA-HD [17]	>400ms	+ no drift during free motion + drift during contact enhances safety at increasing delay	− requires sensing or estimation of external wrench − disadvantages of drift during contacts may overrule its advantages at lower delays
+μ-ER, DDPA *[future work]*		+ μ-ER promises to reduce jitter and force drops on input device side	− DDPA required on robot side to ensure passivity

TABLE I: Benefits and limitations of various TDPA approaches.

of the coupling controller, such that passivity will always be ensured. This will be explained in more detail in Section II.

Table I serves for comparison of advantages and limitations of different TDPA concepts. TDPA-HD is closely related to TDPA, but optimized for high delay, and requires measurement or observation of external forces. Thanks to avoidance of position drift, TDPA-ER shows enhanced coupling rigidity which, however, can also limit performance at high delays. In this work, we transfer the μ-ER approach from TDPA-ER to TDPA involving the deflection-domain passivity approach (DDPA) for passivity guarantee.

In contrast, in TDPA, due to its unidirectional passivity observation and control, it is not trivial to allocate energy information to the input device side presciently while preventing that the respective energy exits to the robot. As a solution to this, in this letter, we present how prescient energy reflection (μ-ER) can be applied to TDPA to reduce force drops (Issue 2.B) as well as jitter (Issue2.A) through a combination with DDPA [25], [26], [21].

The paper is structured as follows: Section II introduces the fundamentals of TDPA and μ-ER. The concept and implementation of the proposed method is presented in Section III. The experimental evaluation in a teleoperation setup with delayed communication is shown in Section IV. The results, limitations and potential future work are discussed in Section V. Finally, Section VI concludes the work.

II. Fundamentals and Problem Statement

This section first describes the principles of the TDPA and the respective artifact of Issue 2 and later how this artifact was solved in TDPA-ER as well as the idea behind the deflection-domain passivity approach.

A. TDPA

The signal flow diagram of a TDPA architecture is presented in Fig. 1. In such a teleoperation setup, a human operator uses an input device to control a robot in its environment. A coupling controller $Ctrl$ compares the reference x^{ref} and robot pose x^{R} and generates a force that pushes the robot to the

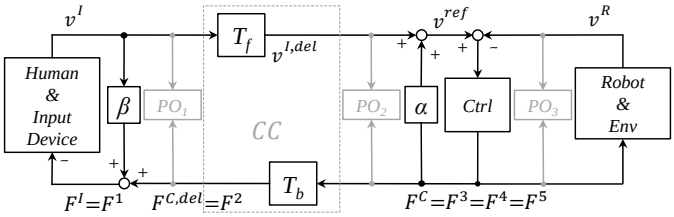

Fig. 1: Signal flow diagram of a TDPA position-force computed architecture with communication delay T_f and T_b. The TDPA involves an impedance-type PC_2 β and an admittance-type PC_1 α.

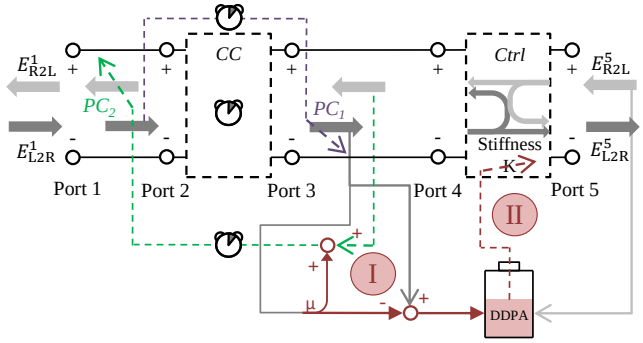

Fig. 2: Proposed enhanced concept for TDPA. The bold arrows indicate the energy flow in the system. Circle I marks the reflection point of the μ-ER method. Circle II marks the DDPA method. Note that the DDPA acts outside the passivity controlled subsystem in contrast to [21].

reference pose, penalizing a position deviation. The passivity observers PO observe the power flow in the system. Note that PO_3 can be neglected for now. The TDPA introduces an admittance-type passivity controller PC_1 with damping α (on the robot side of the communication channel) that dissipates observed excessive energy that has been introduced by a forward delay T_f in left-to-right (L2R) energy flow direction by reducing the velocity command $v^{\text{I,del}}$ to v^{ref}. The impedance-type passivity controller PC_2 with damping β attenuates the force feedback $F^{\text{C,del}}$ to F^1 on the opposite side to dissipate energy that was generated by the delay T_b in right-to-left (R2L) energy flow direction. The reader is referred

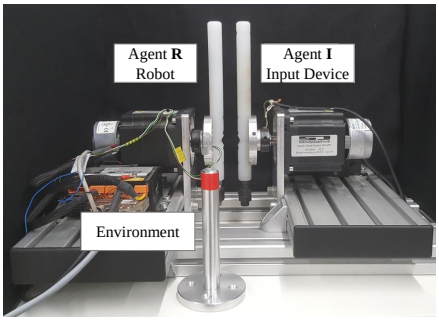

Fig. 3: Experimental Setup: two 1-DoF direct-drive devices.

to [2] for more details on passivity control in TDPA.

The network representation of this setup depicted in Fig. 2 provides ports at which power correlated signals (velocity v and Force F) can be observed to measure the power $P_i(k) = v_i(k)F_i(k)$ in time step k at port i. Regarding the sign of the power, the power flow direction can be determined:

$$P^i_{\text{L2R}}(k) = \begin{cases} 0, & \text{if } P^i(k) \leq 0 \\ P^i(k), & \text{if } P^i(k) > 0, \end{cases} \quad (1)$$

$$P^i_{\text{R2L}}(k) = \begin{cases} 0, & \text{if } P^i(k) \geq 0 \\ -P^i(k), & \text{if } P^i(k) < 0. \end{cases} \quad (2)$$

Note that the sign of the flow direction depends on the sign convention in $Ctrl$. With sampling time T_s, the monotonously increasing energies can be calculated via integration: $E^i_{\text{L2R}}(k) = T_s \sum_{j=0}^{k} P^i_{\text{L2R}}(j)$ and $E^i_{\text{R2L}}(k) = T_s \sum_{j=0}^{k} P^i_{\text{R2L}}(j)$. The methods I and II marked with red circles are not a part of the TDPA, and will be described in Section III.

All following experiments were performed with the hardware depicted in Fig. 3. The controller was implemented in Matlab/Simulink and executed on a rtLinux system at 1kHz. Figures 4 and 5 present experiments with 150 ms and 400 ms RTD respectively (T_f=T_b) with wall contact and subsequent free motion phase. Grey shades mark wall contacts and blue shades mark occurrences of jitter throughout the manuscript. Position drift (Issue 1) is visible from the position plots showing a position offset at $t = 42.5s$ in Fig. 4 and at $t = 7.5s$ in Fig. 5. The force drops and jitter (blue shaded area) are more evident in both experiments. In the course of this work, we analyze system performance based on the metrics F^{δ}_I on force attenuation and K^{per} on perceived stiffness. A lower F^{δ}_I=$\frac{F^2-F^1}{F_2}$ and a higher K^{per}=$\frac{F_1/(x^3-x^5)}{K_{Ctrl}}$ (perceived stiffness closer to K_{Ctrl}) indicate better performance.

Figure 6 presents a simplified abstract delayed teleoperation scenario with input device pose x^I and robot pose x^R. The position drift (Issue 1, which is not the focus of this paper) is caused by PC_1 and visualized by the position offset $p^2 - p^1$ between the input device pose x^I serving as the reference pose of the robot represented by the pose x^R. In this paper, we aim to solve Issue 2.A and Issue 2.B for the TDPA which are caused by the dissipative action of PC_2. Jitter (Issue 2.A) results from passivity control itself since the dissipative action of PC_2 can lead to a change in power flow direction leading to fast iterative activation and deactivation of PC dissipation. Force drop (Issue 2.B) refers to the initial PC_2 dissipation during maximum wall penetration lasting for one RTD.

A significant effect of the drop in force feedback is that the operator (who might have maintained a force against the wall while slowly releasing the wall penetration) potentially drops back into the wall, as an effect of the drop in the force feedback, such that energy is injected inadvertently and the wall penetration is increased instead. This issue and the origin of this Issue 2.B was already discussed in detail in [21], but will be repeated here to ease understanding of the proposed concept. From the beginning of the experiment to maximum wall penetration (t=$[40.2s; 42.2s]$ in Fig. 4, t=$[t_0; t_1]$ in Fig. 6), energy flows in L2R direction since the human moves the robot. At the same time, the power (and energy) that flows in R2L direction P^i_{R2L}=0 is zero on both sides of the communication channel: $P^2_{\text{R2L}}(k)$=0 and $P^3_{\text{R2L}}(k)$=0. When the input device starts releasing the wall contact (from t=$42.2s$ in Fig. 4, t_1 in Fig. 6), first, the velocity sign on the operator side changes, flipping the power flow direction such that suddenly $P^2_{\text{R2L}}(k)\neq 0$ while $P^3_{\text{R2L}}(k)$=0. That means that PC_2 has to completely dissipate the power $P^2_{\text{R2L}}(k)$ through attenuation of the force feedback to ensure passivity of the communication channel in R2L direction until, one RTD later, $P^3_{\text{R2L}}(k-T_b)\neq 0$ (from t=42.2 in Fig. 4, t_3 in Fig. 6). Summarizing, the reason for Issue 2.B is that no energy was sent from the robot side to the operator side in R2L direction before energy is required to leave to the operator side. This leads to intense force drops which become especially visible during wall contacts. Such strong force drops cannot be prevented effectively via filters such as proposed in [2].

B. Preventing Issue 2 in TDPA-ER

In [21], we solved Issue 2 through prescient energy reflection for TDPA-ER (see Fig. 7): A proportion $\mu \in [0, 1]$ of the energy information that arrives on the robot side P^3_{L2R} is directly reflected back to the operator-side passivity controller PC_2 and is there allocated to the energy output to the operator at port 1. To maintain passivity, the reflected power is erased from L2R direction (energy input to monitoring unit multiplied by $1-\mu$) such that the power proportion μP^3_{L2R} may not leave in L2R direction to the robot. The reflected proportion $\mu(t)$ can be designed to depend on the position deviation of input device and robot and/or the velocity of the robot such that energy is reflected only during wall contacts (when power is expected to be reflected back to the input device). Due to the prescient reflection, output power is available at port 1 already during the pressing phase of the wall contact and may exit to the operator in R2L direction as soon as the wall penetration is released. Thus, at adequate velocities, the artifacts of Issue 2.A as well as Issue 2.B could be resolved in TDPA-ER since the passivity control action on the operator side is not triggered at all. For more details, the reader is referred to [21].

The prescient μ-ER is straight forward in TDPA-ER since the passivity controllers surround the communication channel as well as the coupling controller and since energy reflection is already a core part of the original TDPA-ER concept.

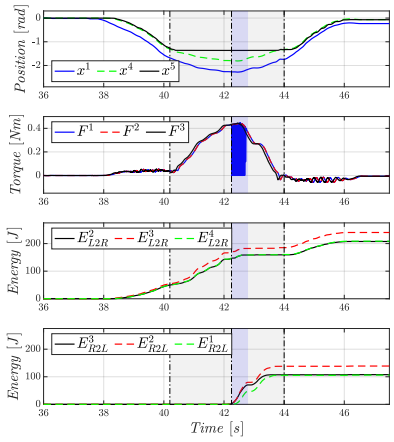

Fig. 4: Performance of TDPA at 150 ms RTD: free motion and wall contact. Force drop (Issue 2.B) is observable starting from maximum of wall penetration t=42.2s. F_I^δ=5.35%, K^{per}=32.3%.

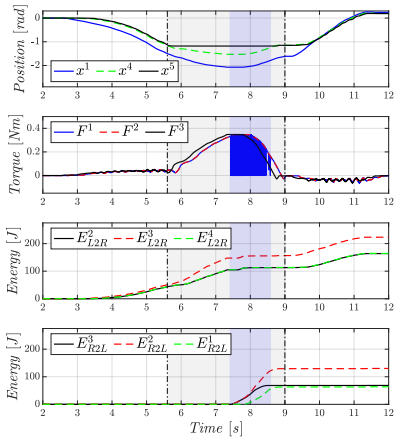

Fig. 5: Performance of TDPA at 400 ms RTD: free motion and wall contact. Force drop (Issue 2.B) is observable starting from maximum of wall penetration $t = 7.4s$ and jitter (Issue 2.A). F_I^δ=15.7%, K^{per}=27.4%.

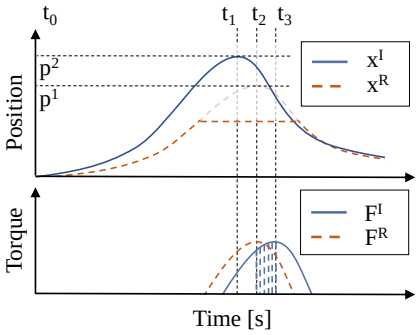

Fig. 6: Abstract visualization of Issue 1 and 2 in a delayed scenario (RTD=$t_3 - t_1$). The vertical dashed force lines mark the time of the force drop (Issue 2.B) during which no power output on the operator side is available yet.

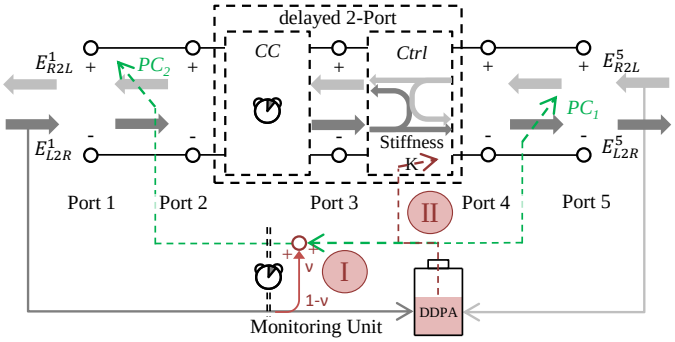

Fig. 7: μ-ER and DDPA in TDPA-ER. In contrast to TDPA, an impedance-type PC is applied on the right side of the $Ctrl$. Since μ-ER and DDPA are located between the two PCs, passivity is intrinsically guaranteed.

Thus, passivity is always maintained. Note that the deflection-domain passivity approach (DDPA), applied also in this work, was already applied in [21] to enhance performance although it is not required to guarantee passivity in TDPA-ER.

In TDPA, energy cannot be directly reflected since the TDPA acts in both flow directions separately. Therefore, we introduce the DDPA into the TDPA framework which allows for indirect attenuation of the coupling controller force in a comparably non-conservative manner via temporary adaptation of the controller stiffness.

C. DDPA

The functionality of the DDPA is presented in Fig. 8. So far, the DDPA was applied to ensure passivity despite variable stiffness [25], [26] or communication delay [21]. Figure 8a shows that, during a wall contact with spring deflection δ=$x^{\text{ref}}-x^R$, potential energy is injected and stored in the coupling controller during the pressing phase of the spring. This energy is released again during the release phase (compare E_{an}). The DDPA is applied if less energy is injected into the coupling controller 2-port $E_{\text{obs}}(k)$=$E^4_{\text{R2L}}(k)$+$E^5_{\text{L2R}}(k)$−$E^4_{\text{L2R}}(k)$−$E^5_{\text{R2L}}(k)$ until δ_{max} than would be expected analytically regarding stiffness K and deflection δ: E_{an}=$\frac{1}{2}K\delta^2$. This can happen if the stiffness was varied during the pressing phase [25] or if energy should not be available on the robot/controller side since it was presciently reflected to the operator side [21].

In simple terms, the DDPA calculates a stiffness profile K_{lim} based on an arbitratry polynomial function $K_{\text{lim}}(\delta)$=$a\delta^d$+$b\delta$+c at maximum spring deflection that ensures that $E_{\text{obs}}(\delta$=$0)\geq 0$ as depicted in Fig. 8b. The observed energy in dependency of the spring deflection can thus be formulated:

$$\begin{aligned} E_{\text{obs}}(\delta) &= \int_0^{\delta} K_{\text{lim}}(\xi)\xi d\xi \\ &= a\frac{1}{d+2}\delta^{d+2} + b\frac{1}{3}\delta^3 + c\frac{1}{2}\delta^2. \end{aligned} \tag{3}$$

Then, the required polynomial K_{lim} ensuring the required energy dissipation can be calculated considering measured values (observed energy $E_{\text{obs}}(\delta_k)$ and stiffness $K(\delta_k)$ at the current deflection $\delta(k)$).

The benefit of energy dissipation in the deflection-domain through DDPA over dissipation in the time domain is that the dissipation happens over the full deflection in a predictive manner and thus comparably early. In contrast, the PCs of the TDPA dissipate energy only when no energy is left (that could exit without violating passivity) such that the force may need to be fully attenuated (resembling zero coupling stiffness). The reader is referred to [25] and [21] for more details on the DDPA. As will be presented later, the early force attenuation resulting from DDPA leads to a comparably low variation of the output force.

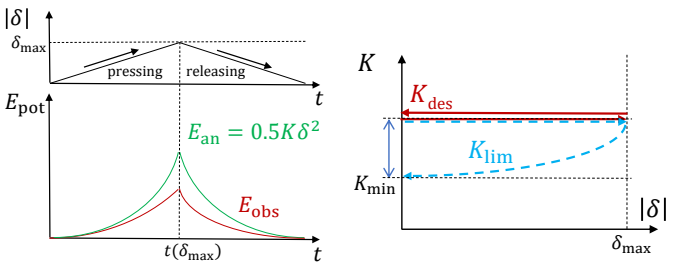

(a) Spring deflection, analytical E_{an}, and observed energy E_{obs}.

(b) Stiffness attenuation to K_{lim} during releasing phase.

Fig. 8: The Deflection-Domain Passivity Approach adapts the stiffness of the coupling controller to limit its energy output. The energy observation happens in time domain whereas the control is designed in the deflection domain.

III. Proposed Approach

As discussed above, Issue 2B is solved here for TDPA through prescient energy reflection along the lines of [21]. While DDPA was applied in [21] solely to improve performance, DDPA is required here to ensure passivity of the overall teleoperation 2-port (between port 1 and port 5). Figure 2 presents module I and II of the proposed concept.

A. Implementation

Module I presents the prescient reflection of a part μ of the energy E^1_{L2R} sent from the operator side to the passivity observer PO_2. It has to be noted that (in contrast to the coupling controller that really reflects energy) this reflection of energy refers only to energy information that is shared with the passivity observer PO_1 feeding the passivity controller PC_2.

Module II marks the action of the DDPA that ensures that energy that should be available to exit on the operator side (which is therefore reflected presciently by Module I) is not available on the robot side. The DDPA thus does not account the reflected proportion of energy E^{μ}=$\mu E^1_{L2R}(k\text{-}T_f)$ in the observed potential energy of the coupling controller:

$$\begin{aligned} E_{\text{obs}}(k) = {} & E^4_{\text{L2R}}(k) + E^5_{\text{R2L}}(k) \\ & - E^5_{\text{L2R}}(k) - E^4_{\text{R2L}}(k) - E^{\mu}(k). \end{aligned} \tag{4}$$

Here, E_{obs} represents the available energy on the robot side represented by the battery symbol in Fig. 2. Note that E_{obs} is updated according to the actual energy output $E^5_{\text{L2R}}(k)$ and $E^4_{\text{R2L}}(k)$ of the Ctrl in (4).

Regarding passivity, the proportion of reflected energy can be chosen arbitrarily. Still, energy has to be available on the robot side especially if the robot is in free motion. In such situations, no energy should be reflected to the human operator. Therefore, the reflected proportion $\mu \in [0, 1]$ can be designed to be variable and depend on the deflection δ of the coupling controller's spring and the speed of the robot as follows:

- The deflection $|\delta|$ should be above a certain threshold δ_{c} when strong reflection is enabled such that only during contacts, a maximum proportion of energy μ_{max} is reflected. To render the detection of a contact more precise, the robot velocity can be considered in addition by activating μ_{max} only if $|v_R|$ is below a threshold v_{c}.

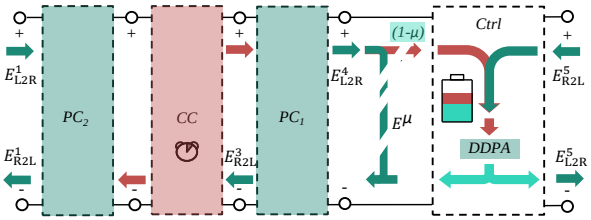

Fig. 9: Active and dissipative components of the enhanced concept for TDPA (analogous to Fig. 2): Passivity controllers are visualized as separate 2-port systems. Red arrows indicate energies leading to passivity violation if not controlled.

- Especially if the delay is low, velocities may be high such that (if δ_c and v_c are chosen too conservatively) too little energy might have been reflected and, thus, Issue 2 not be prevented. Therefore, the minimum proportion μ_{min} of energy that is reflected may be chosen non-zero.
- In highly variable setups, the reflected energy proportion $\mu(\delta, v^R, T_f, T_b)$ may also depend on the communication delay (which is not considered in this work).

B. Passivity Discussion

In addition to the explanations above, a detailed passivity discussion is presented in the following. The scheme of Fig. 9 marks components of the teleoperation network that generate energy (marked in red) and that dissipate energy (marked in green). Note that the dashed energy arrows represent energy information that is required as a reference for passivity control. For instance, not the energy E^{μ}, but only the information on its availability is sent back to the operator. Analogously, not the energy $E^4_{\text{L2R}} - E^{\mu}$ enters the coupling controller, but only its value is handed over to DDPA to inform about the available energy in the coupling controller. Instead, the energy E^4_{L2R} enters the coupling controller. The battery symbol shows the exemplary real energy content of the controller (red filling) and the available energy in the controller (green filling). The DDPA ensures via adaptation of the stiffness that only the available energy exits the controller. Additional energy is injected by the communication channel (therefore marked in red) which is dissipated by the standard passivity controllers of the TDPA.

Analysing the scheme of Fig. 9, it becomes obvious that the DDPA is able to ensure passivity of the overall system: The actual potential energy stored in the Ctrl is

$$E_{act}(k) = E^4_{\text{L2R}}(k) + E^5_{\text{R2L}}(k) - E^5_{\text{L2R}}(k) - E^4_{\text{R2L}}(k). \tag{5}$$

Since $E_{act}(k) \geq E_{obs}$, with E_{obs} defined in (4), the DDPA will always be able to ensure the dissipation of the energy E^{μ} that has been reflected to the input device side, thus ensuring overall passivity.

In fact, the proposed method is more conservative than required by the passivity condition since the DDPA currently doesn't consider that an energy amount that was already reflected via E^{μ} and that is later really reflected by the $Ctrl$ doesn't need to be considered in the DDPA. An improved, less conservative solution should be developed in future work.

Note that alternatively, the energy E^{μ} could already be reflected at port 1, 2 or 3. If reflected at port 2 or 3, the

dissipation would require additional dissipation of PC_1 causing additional position drift if DDPA is not applied. Reflecting energy at port 1 would require more complex calculation of the available energy on the robot side. If energy is reflected already on the left side of the CC, the force drop can be prevented independent of the delay, but an adaptation of μ according to the contact situation is not reasonable since this information would arrive delayed on the input device side. Thus, reflecting energy at port 4 appears to be optimal while a more detailed comparative study remains for future work.

IV. Experimental Evaluation

Analogous to the preceding experiments, the following were performed with the setup of Fig. 3. Figure 10 to 12 present wall contacts at different delays while the proposed method was activated. The μ parametrization was adapted manually according to the delay.

In the following experiments, we adapt μ according to the spring deflection δ:

$$\mu(k) = \begin{cases} \mu_{min}, & \text{if } |\delta| < \delta_c, \\ \mu_{max}, & \text{if } |\delta| \geq \delta_c, \end{cases} \tag{6}$$

considering a threshold of $\delta_c = 0.03rad$.

The first experiment and the first wall contact of Fig. 11 correspond with the experiments with pure TDPA of Fig. 4 and Fig. 5. Analyzing the force plot, it is obvious that, due to adequate speeds, the force drop (Issue 2.B) and jitter (Issue 2.A) are completely prevented (although passivity controllers were enabled) through the μ-ER approach while overall passivity is maintained: $E_{\text{PP}}^{1-5}>0$. This is achieved through adaptation of the stiffness to K_{lim} by up to 50% which leads to a still comparable low attenuation of the force during the release phase of the wall contact: F_{Ctrl} is the force which would result from a constant $K_{Ctrl} = 1Nm/rad$. Although the attenuation is visible, the approach promises to improve the user experience when compared to pure TDPA since the force profile is close to the one of a conventional spring with constant stiffness. The clearance between energy plots $E_{\text{R2L}}^3 + E_\mu$ and E_{R2L}^2 indicates that the μ-value could have been reduced in case of 150ms RTD but should be further increased at 800ms RTD to increase the robustness and to avoid dissipation via PC_2.

Fig. 11 presents the performance at varying velocities. As expected, increasing release velocities (contact 1 versus contact 2) don't provoke jitter, while increasing pressing velocities (contact 3) increase Issue 2.A and 2.B. Since contact 4 is faster than one RTD, position drift is high and K_{lim} and F^2 are particularly low.

The experiment depicted in Fig. 13 serves the evaluation of robustness in case of contacts with movable objects. For this sake, the robot is first controlled with large forces into contact with an object, which is removed at t=15.5s. Although a proportion of the energy was reflected to the user due to μ-ER, the robot is moving unrestrictedly to the reference pose x^4 showing that the μ-ER is able to handle dynamic environments thanks to the incorporation of DDPA on the robot side. At t=19s, the operator moves back to the initial pose while the robot is held back first until it is released at t=22.7s. During this specific procedure, the PC_1 is triggered since the robot overshoots the reference pose, sending additional energy to the operator side. The origin of this artifact is explained in more detail in the following experiment.

Figure 14 depicts the system behavior in case of active environments. When, for instance, a human in the robot's environment moves the robot, energy flows in R2L direction from robot to operator. In this case, no force drop (Issue 2.B) appears due to PC_2 since the energy information arrives at the same time as the energy itself on the operator side. Still, since no energy information may be reflected presciently, jitter (Issue 2.A), resulting from PC_2 dissipation of the energy injected by the communication delay, cannot be prevented. It should be noted that a position-force architecture is not the optimal choice for scenarios with active environments. In setups involving active components on both sides of the communication channel, a position-position architecture [27], [22] or additional methods inducing plastic reactions particularly to active environments [23] are favourable.

The experiment in Fig. 15 on the enhanced TDPA-ER [21] applying μ-ER and DDPA allows for a performance comparison with the proposed extension of TDPA at same delay and μ-settings in Fig. 11. Since TDPA-ER is free of position-drift, a high coupling rigidity is achieved as confirmed by K^{per}. Still, the higher coupling rigidity of TDPA-ER is beneficial at lower delays, but potentially limits perception at higher delay. At increasing pressing velocities (contact 2 and 3 in Fig. 15) jitter appears already at lower velocities than in case of TDPA.

V. Discussion and Limitations

The experiments confirmed that the μ-ER approach is able to prevent force drops and jitter in standard teleoperation scenarios. Still, it has to be considered that the effectiveness of the approach depends on the motion speed of the operator. If the operator moves too fast regarding the prevalent delay, no energy information may have been reflected and arrived on the operator side, before energy tries to exit to the operator. Choosing $\mu_{min}\neq 0$ can help providing available energy on the operator side in time, but may reduce the free motion tracking performance of the robot. An alternative, that should be studied in future work, would be the reflection of energy flowing in L2R direction already on the operator side at port 2. Thereby, it should be evaluated if the reflected energy, which should not be available on the robot side, can be considered by the DDPA such that it does not lead to position drift caused by PC_1 dissipation.

The present evaluation is limited to a 1-DoF scenario. Since TDPA [17] and DDPA [26] are functional in 6-DoF, the extendability of the proposed method to multi-DoF can be assumed but remains to be confirmed.

The metrics F_I^δ and K^{per} confirmed that the force is less attenuated and that the perceived stiffness is not altered significantly more by DDPA when compared to pure TDPA. Comparing TDPA with TDPA-ER, it can be observed that TDPA-ER achieves higher perceived stiffnesses, but is more sensitive to inadequate velocities regarding the delay range.

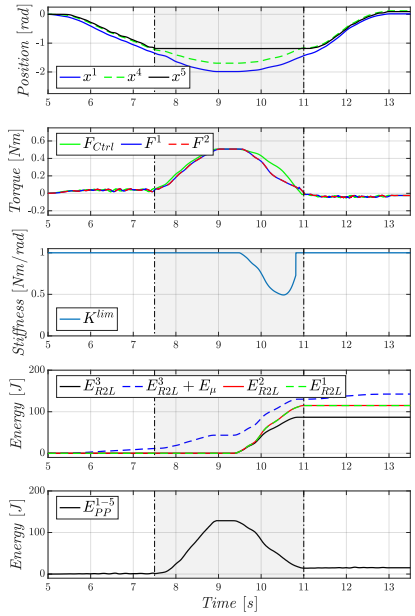

Fig. 10: μ-ER TDPA at 150 ms RTD: $\mu_{\min}$=$\mu_{\max}$=0.25. Due to appropriate velocity and μ-ER, no force drops and jitter appear. The adaptation of the force F_K to F_3 is comparably low. F_I^{δ}=0%, K^{per}=45.8%.

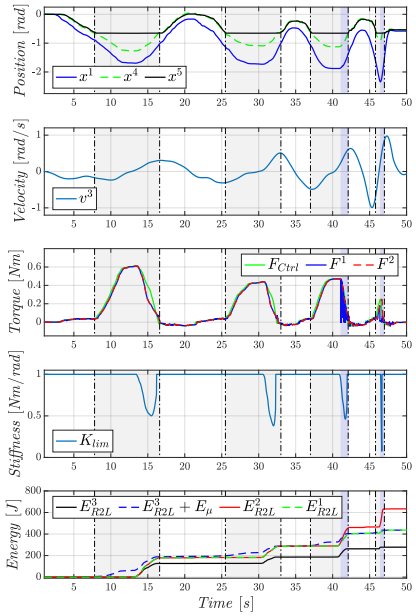

Fig. 11: μ-ER TDPA at 400 ms RTD: $\mu_{\min}$=0, $\mu_{\max}$=0.3. Varying pressing and release velocities during wall contacts. F_I^{δ}=[0%,0%,5.3%,58.3%], K^{per} = [38.8%, 27.4%,28.1%,7.5%].

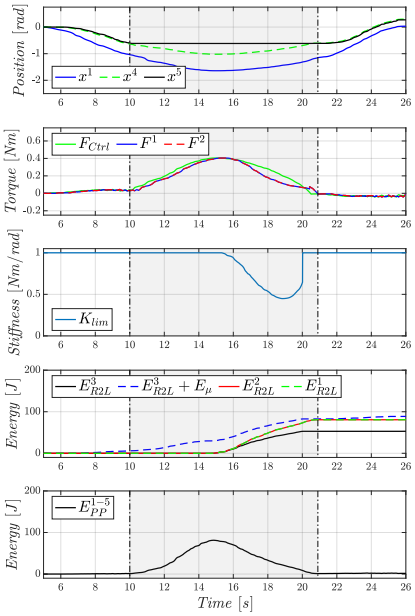

Fig. 12: μ-ER TDPA at 800 ms RTD: $\mu_{\min}$=0, $\mu_{\max}$=0.3. Due to velocities adapted to the delay range, performance comparable with the experiment at 150ms RTD. F_I^{δ}=0%, K^{per}=23.6%.

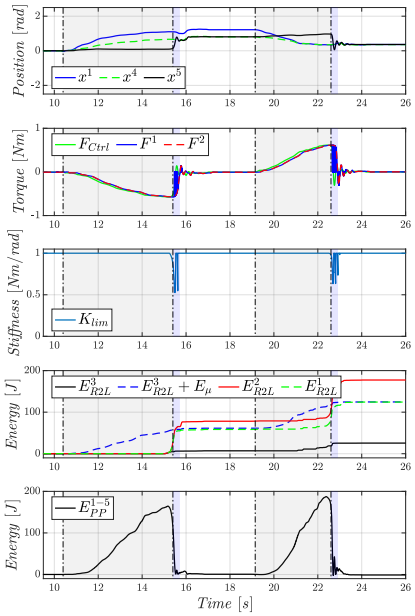

Fig. 13: μ-ER TDPA at 400 ms RTD: $\mu_{\min}$=0, $\mu_{\max}$=0.3. The object suddenly evades the interaction. Jitter appears since $E^2_{R2L} > E^3_{R2L} + E_\mu$.

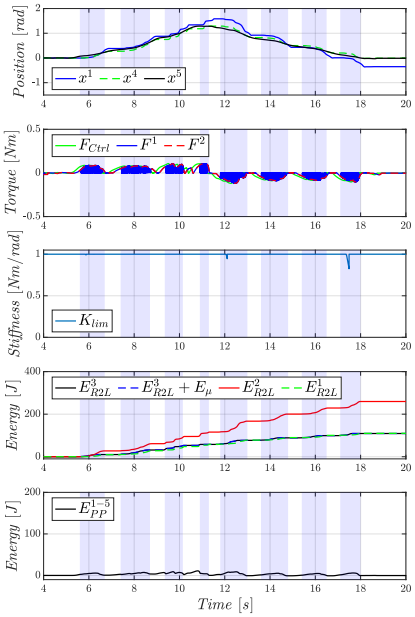

Fig. 14: μ-ER TDPA at 400 ms RTD: $\mu_{\min}$=0, $\mu_{\max}$=0.3. In case of active environments, μ-ER cannot reflect energy prescienlty to avoid jitter.

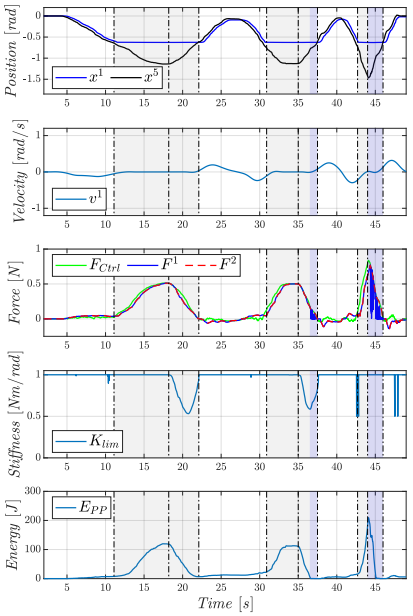

Fig. 15: μ-ER TDPA-ER at 400 ms RTD: $\mu_{\min}$=0, $\mu_{\max}$=0.3. As for TDPA, the pressing velocity has to be adapted to the delay. F_I^{δ}=[0%,2.8%,20.9%], K^{per}=[87%,81.5%,50%].

As discussed based on Table I, a rigid coupling is beneficial at low delays, but may have negative aspects at higher delay. Therefore, transferring μ-ER to TDPA-HD in a next step to increase performance at high delay ranges is essential.

Another noteworthy difference between conventional TDPA and methods involving prescient energy reflection becomes obvious when analyzing the respective jitter properties. Prescient energy reflection does not only reduce the jitter duration but also the force jumps within. In case of conventional TDPA, the force changes mostly more than 50% during phases of jitter ($>90\%$ of all force jumps during jitter phases) which is well perceivable by the operator since no or negligible energy (Issue 2.B) is available. In contrast, the force jumps are less pronounced ($<50\%$ of all force jumps during jitter phases) and thus potentially less perceivable if prescient energy reflection is applied in TDPA or TDPA-ER respectively since at least a proportion of the required energy is available.

Also, future work should investigate strategies for adaptation of the μ reflection proportion. Machine learning methods can be applied to study if consideration of the robot velocity and power flow brings benefits in μ adaptation.

Currently the DDPA acts independent of the energy flow direction. Despite the significantly enhanced performance, future work may evaluate if the approach can be rendered less conservative by considering that energy that is finally reflected by the coupling controller does not need to be limited by DDPA.

VI. Conclusion

This paper transferred the μ-ER method developed for enhanced force transparency in TDPA-ER to TDPA to presciently reflect an adaptive proportion μ of energy sent from the operator (to the robot side) back to the operator side. It was shown that at adequate speeds and in passive environments, μ-ER can prevent drops and jitter in the force feedback that originally resulted from the dissipative action of the operator-side impedance-type passivity controller. The deflection-domain passivity approach was applied to maintain passivity of the overall teleoperation 2-port. The energy dissipation induced by this approach has been shown to result in comparably low and particularly smooth force attenuation. As confirmed by the metrics F_I^δ and K^{per}.

The major research that needs to be investigated in future work are the extension of the approach to SO(3) and the adaptation of the proposed method to TDPA-HD.

References

[1] G. D. Niemeyer, "Using wave variables in time delayed force reflecting teleoperation," Ph.D. dissertation, MIT, 1996.

[2] J.-H. Ryu, J. Artigas, and C. Preusche, "A passive bilateral control scheme for a teleoperator with time-varying communication delay," *Mechatronics*, vol. 20, no. 7, pp. 812–823, 2010.

[3] M. Franken, S. Stramigioli, S. Misra, C. Secchi, and A. Macchelli, "Bilateral telemanipulation with time delays: A two-layer approach combining passivity and transparency," *IEEE transactions on robotics*, vol. 27, no. 4, pp. 741–756, 2011.

[4] M. Jorda, M. Vulliez, and O. Khatib, "Local autonomy-based haptic-robot interaction with dual-proxy model," *IEEE Transactions on Robotics*, vol. 38, no. 5, pp. 2943–2961, 2022.

[5] J.-H. Ryu and C. Preusche, "Stable bilateral control of teleoperators under time-varying communication delay: time domain passivity approach," in *IEEE International Conference on Robotics and Automation*. IEEE, 2007, pp. 3508–3513.

[6] J. Rebelo and A. Schiele, "Time domain passivity controller for 4-channel time-delay bilateral teleoperation," *IEEE transactions on haptics*, vol. 8, no. 1, pp. 79–89, 2014.

[7] D. Sun, F. Naghdy, and H. Du, "Neural network-based passivity control of teleoperation system under time-varying delays," *IEEE transactions on cybernetics*, vol. 47, no. 7, pp. 1666–1680, 2016.

[8] J.-H. Ryu, D.-S. Kwon, and B. Hannaford, "Control of a flexible manipulator with noncollocated feedback: time domain passivity approach," in *Control Problems in Robotics*. Springer, 2003, pp. 121–134.

[9] R. Balachandran, H. Mishra, M. Panzirsch, and C. Ott, "A finite-gain stable multi-agent robot control framework with adaptive authority allocation," in *2021 IEEE ICRA*. IEEE, 2021, pp. 1579–1585.

[10] H. Van Quang and J.-H. Ryu, "Stable multilateral teleoperation with time domain passivity approach," in *International Conference on Intelligent Robots and Systems*. IEEE, 2013, pp. 5890–5895.

[11] M. Panzirsch, T. Hulin, J. Artigas, C. Ott, and M. Ferre, "Integrating measured force feedback in passive multilateral teleoperation," in *Haptics: Perception, Devices, Control, and Applications*. Springer, 2016, pp. 316–326.

[12] H. Singh, M. Panzirsch, and J.-H. Ryu, "Preserving the physical coupling in teleoperation despite time delay through observer-based gradient control," *IFAC-PapersOnLine*, vol. 52, no. 18, pp. 25–30, 2019.

[13] M. Panzirsch, J.-H. Ryu, and M. Ferre, "Reducing the conservatism of the time domain passivity approach through consideration of energy reflection in delayed coupled network systems," *Mechatronics*, vol. 58, pp. 58–69, 2019.

[14] X. Xu and E. Steinbach, "Elimination of cross-dimensional artifacts in the multi-dof time domain passivity approach for time-delayed teleoperation with haptic feedback," in *2019 IEEE World Haptics Conference (WHC)*. IEEE, 2019, pp. 223–228.

[15] A. Coelho, H. Singh, T. Muskardin, R. Balachandran, and K. Kondak, "Smooth position-drift compensation for time domain passivity approach based teleoperation," in *Intelligent Robots and Systems (IROS), 2015 IEEE/RSJ International Conference on*. IEEE, 2018.

[16] X. Xu, C. Schuwerk, B. Cizmeci, and E. Steinbach, "Energy prediction for teleoperation systems that combine the time domain passivity approach with perceptual deadband-based haptic data reduction," *IEEE transactions on haptics*, vol. 9, no. 4, pp. 560–573, 2016.

[17] M. Panzirsch, A. Pereira, H. Singh, B. Weber, E. Ferreira, A. Gherghescu, L. Hann, E. den Exter, F. van der Hulst, L. Gerdes *et al.*, "Exploring planet geology through force-feedback telemanipulation from orbit," *Science Robotics*, vol. 7, no. 65, 2022.

[18] J. Artigas, J.-H. Ryu, and C. Preusche, "Position drift compensation in time domain passivity based teleoperation," in *IEEE/RSJ IROS*. IEEE, 2010, pp. 4250–4256.

[19] V. Chawda and M. K. O'Malley, "Position synchronization in bilateral teleoperation under time-varying communication delays," *Ieee/asme transactions on mechatronics*, vol. 20, no. 1, pp. 245–253, 2014.

[20] X. Xu, M. Panzirsch, Q. Liu, and E. Steinbach, "Integrating haptic data reduction with energy reflection-based passivity control for time-delayed teleoperation," in *2020 IEEE Haptics Symposium (HAPTICS)*. IEEE, 2020, pp. 109–114.

[21] M. Panzirsch, H. Singh, X. Xu, A. Dietrich, T. Hulin, E. Steinbach, and A. Albu-Schaeffer, "Enhancing the force transparency of the energy-reflection-based time-domain passivity approach," *IEEE Transactions on Control Systems Technology*, 2024.

[22] M. Panzirsch and H. Singh, "Position synchronization through the energy-reflection based time domain passivity approach in position-position architectures," *IEEE RAL*, vol. 6, no. 4, pp. 7997–8004, 2021.

[23] M. Panzirsch, H. Singh, X. Wu, I. Maged *et al.*, "Virtual elasto-plastic robot compliance to active environments," *Science Robotics*, vol. 11, no. 99, 2025.

[24] H. Singh, M. Panzirsch, R. Balachandran, J.-H. Ryu, C. Ott, and T. Hulin, "Perceptual-based method for mitigating force chattering in time domain passivity approach," in *2025 IEEE World Haptics Conference (WHC)*. IEEE, 2025.

[25] M. Panzirsch, M. Sierotowicz, R. Prakash, H. Singh, and C. Ott, "Deflection-domain passivity control of variable stiffnesses based on potential energy reference," *IEEE RAL*, vol. 7, no. 2, pp. 4440–4447, 2022.

[26] M. Panzirsch, H. Singh, M. Sierotowicz, and A. Dietrich, "Extension of the deflection-domain passivity approach for variable stiffnesses to so (3)," *IEEE Robotics and Automation Letters*, 2024.

[27] J. Artigas, J.-H. Ryu, and C. Preusche, "Time domain passivity control for position-position teleoperation architectures," *Presence*, vol. 19, no. 5, pp. 482–497, 2010.